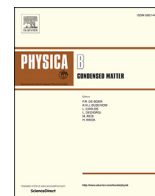


Contents lists available at ScienceDirect

Physica B: Condensed Matter

journal homepage: www.elsevier.com/locate/physb

Neutron imaging with fission and thermal neutrons at NECTAR at MLZ

M.J. Mühlbauer^{a,b,*}, T. Bücherl^c, M. Kellermeier^d, M. Knapp^{a,e}, M. Makowska^{b,f}, M. Schulz^d,
S. Zimnik^{a,b}, H. Ehrenberg^{a,e}^a Institute for Applied Materials (IAM), Karlsruhe Institute of Technology (KIT), Hermann-von-Helmholtz-Platz 1, 76344 Eggenstein-Leopoldshafen, Germany^b Heinz Maier-Leibnitz Zentrum (MLZ), Lichtenbergstr. 1, 85748 Garching, Germany^c Technische Universität München, ZTWB Radiochemie München RCM, Walther-Meißner-Str. 3, 85748 Garching, Germany^d Heinz Maier-Leibnitz Zentrum (MLZ), Technische Universität München, Lichtenbergstr. 1, 85748 Garching, Germany^e Helmholtz Institute Ulm for Electrochemical Energy Storage (HIU), Helmholtzstrasse 11, 89081 Ulm, Germany^f University of Bayreuth, Universitätsstraße 30, 95447 Bayreuth, Germany

ARTICLE INFO

Keywords:

Neutron
Imaging
Thermal
Fission
NECTAR
MEDAPP

ABSTRACT

The instrument NECTAR is located at beam port SR10 of the neutron source FRM II at the Heinz Maier-Leibnitz Zentrum (MLZ). With a pair of moveable uranium plates placed in front of the entrance window of the beam tube, a fission neutron spectrum with a mean energy of 1.9 MeV can be used for neutron imaging applications. Via remote control these plates can be removed and a thermal neutron spectrum (mean energy at 28 meV) gets available for experiments. While the fission neutron spectrum is regularly used, some upgrades of the instrument are necessary to make the thermal neutron spectrum routinely available for user experiments. This includes additional equipment like a new sample stage and a second detector system foreseen to extend the capabilities of NECTAR. The current state of the instrumentation and necessary changes for the future thermal beam option and its usage for standard user experiments will be presented. First measurements were carried out with a temporary flight tube installed and a compact detector (510 mm × 180 mm × 180 mm) for thermal neutrons with a spatial resolution in the range of 100 μm. The feasibility of the thermal beam option could already be verified at an L/D ratio of 240 and a thermal neutron flux of $7.92 \cdot 10^6 \text{ cm}^{-2} \text{ s}^{-1}$. The thermal neutron beam option adds a pure thermal neutron spectrum – Maxwell spectrum originating from the moderator without alteration by a secondary source or converter – to the energy ranges available for neutron imaging at MLZ instruments. It also offers a unique possibility to combine two quite different neutron energy ranges at a single instrument including their respective advantages. The thermal neutron beam option is funded by BMBF in the frame of research project 05K16VK3.

1. Introduction

The primary goal of the project is to provide a pure thermal neutron beam for neutron radiography and tomography measurements at the MLZ. Pure thermal beam in this sense means a Maxwell spectrum originating from the heavy water moderator, which is not altered by any secondary source or converter in front of the beam tube. This extends the available spectral range for neutron imaging in addition to the existing radiography and tomography facilities ANTARES [1] located at a beam port of the cold source and NECTAR [2,3] currently using a fission neutron beam only. The thermal option at NECTAR results in a quite unique possibility for combined experiments with a pure thermal neutron spectrum and a fission neutron spectrum at a single instrument.

Combination of thermal radiography and tomography data with fission neutron imaging promises to give additional contrast especially for hydrogen, while thermal neutron tomography can provide more detailed information about sample dimensions due to higher spatial resolution. In that case the limited spatial resolution for fission neutron radiography and tomography is complemented by data gained with thermal neutrons, which may then be used for instance for mapping the hydrogen distribution in fuel cells or hydrogen storage materials. The other way round, fission neutron data, e.g. a hydrogen distribution, could be used for scattering corrections during the data evaluation of imaging data acquired with thermal neutrons, thus improving the reconstruction results. As the converter plates at the tip of the neutron beam tube SR10 may be removed via remote control, it is possible to simply switch between the

* Corresponding author. Institute for Applied Materials (IAM), Karlsruhe Institute of Technology (KIT), Hermann-von-Helmholtz-Platz 1, 76344 Eggenstein-Leopoldshafen, Germany.
E-mail address: martin.muehlbauer@frm2.tum.de (M.J. Mühlbauer).

<https://doi.org/10.1016/j.physb.2017.11.088>

Received 31 August 2017; Received in revised form 27 November 2017; Accepted 30 November 2017

Available online xxx

0921-4526/© 2017 The Authors. Published by Elsevier B.V. This is an open access article under the CC BY-NC-ND license (<http://creativecommons.org/licenses/by-nc-nd/4.0/>).

fission neutron spectrum and the thermal neutron spectrum. The main components of the existing instrument are kept unchanged and only slight modifications at beam port SR10 are necessary to make the thermal option available for routine operation: the installation of a temporary flight tube and the upgrade of a B_4C filter to make it movable. A preliminary installation of a simple aperture system for thermal neutrons, an evacuated flight tube and a compact detector for thermal neutrons at NECTAR made it possible to carry out first tests and flux measurements. In its final state the thermal beam option at NECTAR is expected to reach characteristic instrument parameters which are comparable to average values of existing state-of-the-art radiography facilities worldwide [4].

Changes for the future thermal beam option and the instrument design are described in the following sections. This includes equipment, which is foreseen to extend the capabilities of NECTAR, e.g. upgrade of the existing detector and a second high resolution detector with a designated sample stage. First data have been acquired with a temporary flight tube and preliminary detector to verify the feasibility of the thermal beam option.

2. Proposed experimental setup

NECTAR (technical tomography) shares the beam port SR10 with MEDAPP (patient treatment and material testing) [5], which is primarily built for medical treatment of malignant tumors. But its irradiation room is also used for biological research and technical irradiation. The layout of the two instruments NECTAR and MEDAPP is shown in Fig. 1. Neutrons are produced by fission of ^{235}U inside the reactor core. After moderation by heavy water a thermal neutron spectrum enters the front window of beam tube SR10. At this position thermal neutrons may trigger the production of fission neutrons by a pair of converter plates containing 500 g of ^{235}U , when these converter plates are moved into their operating position at the tip of the beam tube SR10. After passing the instrument shutters and a series of movable filters mounted on a filter bench, these fission neutrons are available inside the irradiation room of MEDAPP or at the sample position of NECTAR [2,3,5]. With the converter plates at their stand-by position (165 cm away from their operating position) and a B_4C filter removed, it is possible to irradiate samples with a pure thermal neutron spectrum. Currently this B_4C filter is at fixed

position and has to be removed manually, which is only possible by removing a heavy shielding block (≈ 5 t) using a special, hydraulic low lift platform truck in order to get access to the filter bench. This is time-consuming and associated with work to be carried out at elevated dose rate. Therefore, this thermal filter is to be installed on the filter bench combined with one of the moveable filters used for medical irradiation. These filters are positioned by an electro-pneumatic drive and can be removed remotely. Thus, mounting the B_4C filter on one of them in combination with the motorized converter plates will allow for easy switching between the fission and the thermal neutron spectrum in the NECTAR-mode of the instrument. This is done without restrictions of any kind in MEDAPP-mode, as the position of the B_4C filter is still checked by a designated control system via redundant position feedback. That way it is ensured that the B_4C in combination with other compulsory filters is engaged for medical applications.

A modular collimator offering apertures of different minimum diameters is proposed to replace the current collimator with a fixed opening. It allows for a compact design yet making several different L/D ratios available. A sketch of the basic concept is shown in Fig. 2a. Additional filter elements, e.g. Pb or Cd, placed inside or between the main collimator modules would result in an even more flexible collimator system including capabilities of e.g. a multi-filter [6].

In order to prevent flux losses caused by air scattering and to minimize the risk of activation of equipment, a flight tube (Fig. 2b and c) has to be temporarily installed in the MEDAPP irradiation room, either evacuated or filled with helium. The flight tube has to be movable, as it has to be removed for treatment of patients at MEDAPP. A single person should be able to install or remove it without any additional equipment.

The proposed foldable design (cf. Fig. 2b and c) offers an option for a compact storage of the flight tube. Beam limiters should be installed already inside or in combination with the flight tube to adjust the beam size to the sample size and to cut the penumbra region of the beam, thus further reducing possible activation of equipment and other components.

Recently, the detector system was upgraded by additional exchangeable scintillators for detection of either thermal or fission neutrons. For detection of thermal neutrons $^6\text{LiF}/\text{ZnS}$ scintillators with 100 μm , 200 μm and 300 μm thickness are used. Fission neutrons are detected by a PP/ZnS scintillator of 2.4 mm thickness. The installation of a

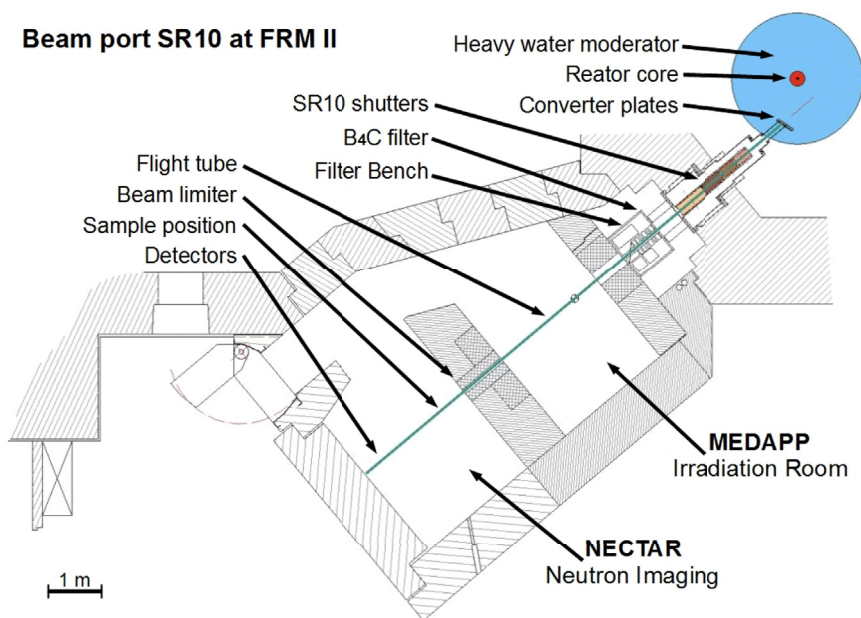


Fig. 1. Present layout of the MEDAPP and NECTAR facilities at beam port SR10 at the neutron source FRM II.

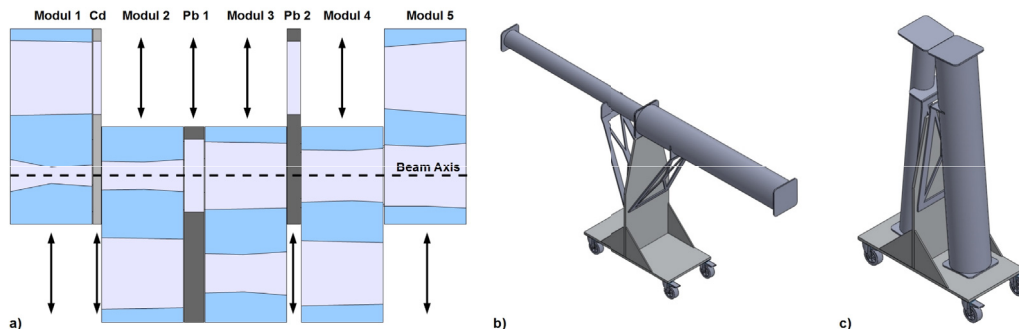


Fig. 2. a) Collimator with movable modules (Modul 1 to Modul 5) enabling for different L/D ratios and additional filters (e.g. Cd, Pb 1, Pb 2) directly included inside the modular collimator; b) proposed layout of a flight tube in operating position, temporarily placed inside the MEDAPP chamber; c) flight tube in storage position.

new CCD camera offering 2048×2048 pixels resulted in reduced pixels sizes for FOVs from about $25 \times 25 \text{ cm}^2$ to a maximum of $40 \times 40 \text{ cm}^2$, at least for thermal neutron applications this results in a higher spatial resolution. For smaller samples, dimensions ranging from 10 cm to 20 cm, a second detector system with smaller fields of view is under construction. It will be optimized for thermal neutron imaging initially equipped with ${}^6\text{LiF}/\text{ZnS}$ scintillators of 100 μm and 200 μm thickness. Thinner ones will be added later to complete the set. Due to these exchangeable scintillators it will offer state-of-the-art spatial resolution for thermal neutrons. But it may also be used for fission neutron imaging with an appropriate scintillator, although the spatial resolution will be limited due to its much larger thickness. In order to reduce the background radiation at the CCD camera a double-mirror system is considered here, similar to the one installed at ANTARES [1]. An additional CMOS camera with faster readout will be available for time resolved studies, when processes have to be studied with single second time resolution. It will be mounted in exchange for one of the CCD cameras inside the two detectors.

3. Experimental proof of concept

First imaging experiments using thermal neutrons at NECTAR were performed with a preliminary setup. The B_4C filter at the exit of the beam tube SR10 was manually replaced by a simple aperture of 25 mm in diameter. The L/D ratio calculated from the diameter and the distance to the sample position was 240. The tests were performed using an evacuated flight tube with a length of 4 m and an outer diameter of 100 mm. Borated rubber installed inside the flight tube acted as an internal beam limiter and reduced activation of the flight tube and production of high energy, secondary gamma radiation. Therefore, the beam size at the sample position was limited to the remaining inner diameter of the flight tube of 85 mm. A compact detector (510 mm \times 180 mm \times 180 mm) for thermal neutrons, the so-called DELCam, was provided by the MLZ in-house detector lab. It is the successor of the prototype described in Ref. [7] and consists of a CCD camera (768 \times 512 pixels) and an optical box with single-mirror layout for imaging the scintillator. In standard configuration it offers a field of view (FOV) of 98.3 mm times 65.5 mm, corresponding to a pixel size of 128 μm . By changing the optical magnification using a lens of 50 mm focal length instead of 25 mm the pixel size was reduced to 57 μm resulting in a FOV of 44.8 mm times 29.2 mm. The CCD sensor was cooled to -31°C . Radiographs of a Cd-edge and a M5 stainless steel screw were acquired using an exposure time of 10 s per frame in order to check the detector resolution and its correct operation. Then a neutron tomography data set was recorded of a Li-ion battery; standard size 18650, 18 mm in diameter and a length of 65 mm. The exposure time of each image was 40 s and two images were taken for each of the 400 angular steps over 360° rotation. Corresponding dark frames and open beam images were used for correction and normalization of all the data.

The thermal neutron flux at the sample position of NECTAR was determined by Au-foil activation. Three foils were irradiated for 3600 s. One of the foils had been covered by a Cd-foil of 1 mm thickness. This measurement provides the so-called Cd-ratio, which is a reference for the epithermal contribution to the neutron spectrum.

4. Results

The spatial resolution was determined by the edge spread function of a Cd edge to be 88.2 μm (5.66 lp/mm) in direct contact to the scintillator. For a sample to detector distance of 28 cm the spatial resolution was reduced to 569 μm (0.88 lp/mm), which is reasonable since the available L/D ratio should add a blurring of around 580 μm due to the large sample to detector distance. Still the resulting spatial resolution is comparable to the maximum resolution achieved by fission neutrons. Thus, thermal neutrons can add geometric information to fission neutron data sets even if samples have to be placed far from the detector due to their size. With the new collimator installed, higher L/D ratios will be available for future experiments, allowing for less geometric blur at least for thermal neutrons, where different thicknesses of the scintillation screens will offer a detector resolution matching the chosen L/D ratio.

Fig. 3 shows a comparison of a raw image, median filtered images of a series of 3, 5, 7 or 9 single images and the final image of the M5 screw normalized to the open beam profile. All images were acquired using the thermal neutron beam. For the given exposure time of only 10 s, a high contamination of gamma spots is observed (Fig. 3a), although the detector had been shielded. The new and upgraded detectors for NECTAR will use improved shielding to reduce the amount of gamma spots. These gamma spots are efficiently removed by filtering a series of 5 images (Fig. 3c). The noise, radiographic mottle, can further be reduced by increasing the number of filtered images (Fig. 3d and e), therefore, allowing for better contrast and higher resolution.

The neutron tomography of the Li-ion battery (standard size 18650) is shown in Fig. 4. It allows a direct comparison of the three dimensional reconstruction with data sets taken at the ANTARES facility [1] with a cold/thermal neutron beam and at the instrument SPODI [8] using a monochromatic neutron beam with a wavelength of 1.548 \AA . From previous measurements it is known that this kind of battery shows an increase of the reconstructed attenuation from the center of the cell to the outside. This increase is due to beam hardening, which was directly proven by the monochromatic tomography carried out at SPODI [9], because it resulted in a flatter profile of the reconstructed attenuation values in radial direction (Fig. 4a). The thermal neutron flux at NECTAR is higher than the flux at SPODI and enables for better signal statistics compared to the monochromatic beam. As a consequence, the data acquired at SPODI are noisier, especially at the center of the cell, than the ones taken at ANTARES or NECTAR, which are of comparable statistics (Fig. 4b).

Due to the thinner scintillation screen (10 μm $\text{Ga}_2\text{O}_2\text{S}$) used for the

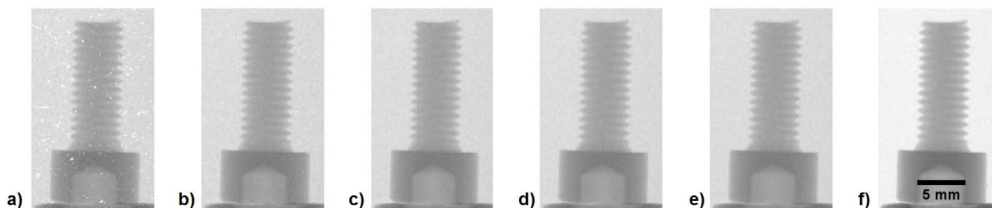


Fig. 3. Radiographies of a M5 stainless steel screw acquired at NECTAR using thermal neutrons: a) raw image, b) median filtered image series of 3 images, c) 5 images, d) 7 images, e) 9 images and f) normalized image. High contamination by gamma spots in the raw image (a), but sufficiently removed by filtering a series of 5 images (c), further reduction of noise by increasing the number of filtered images (d,e).

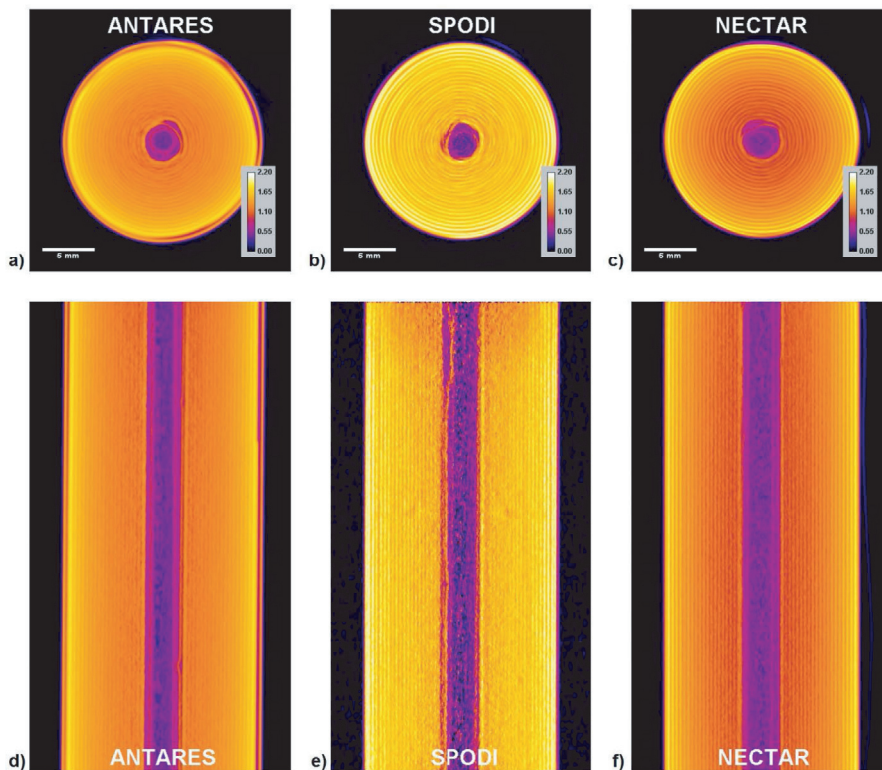


Fig. 4. Reconstructed slices a) to c) and vertical cuts d) - f) through neutron tomography data of a 18650 Li-ion cell. Data have been acquired using a cold/thermal neutron spectrum (ANTARES), monochromatic neutrons (SPODI) and a pure thermal neutron spectrum (NECTAR). Beam hardening is not observed for the SPODI data, but due to the low neutron flux noise is limiting the contrast and resolution at the center of the cell.

measurements at NECTAR, the overall spatial resolution exceeds the one carried out at ANTARES, where a $^6\text{Li}/\text{ZnS}$ scintillator of $100\ \mu\text{m}$ thickness was used, while the pixel size was comparable. Thus, the single layers of electrodes inside the battery show higher contrast for the NECTAR data, especially at the center part of the cell. A second reason for this effect might be a higher neutron transmission due to the higher average neutron energy using the thermal neutron beam at NECTAR compared to the cold/thermal spectrum available at ANTARES, where in this case the cold part of the spectrum does not contribute to the transmission signal significantly due to its higher attenuation. But it contributes to the observed beam hardening and causes a major part of the sample activation. The missing contribution of the cold spectral range at NECTAR does effectively reduce the activation of the samples.

Based on the measured open beam intensities at SPODI and NECTAR the thermal neutron flux at NECTAR was estimated to be $10^7\ \text{cm}^{-2}\text{s}^{-1}$. From Au-foil activation the integral thermal neutron flux at the sample position of NECTAR has been determined to be $7.92 \cdot 10^6\ \text{cm}^{-2}\text{s}^{-1}$ when

an average neutron wavelength of $1.81\ \text{\AA}$ is assumed for the beam. The value of the epithermal contribution results from the activation of the foil covered by a Cd-filter of $1\ \text{mm}$ thickness and is calculated to be $1.05 \cdot 10^6\ \text{cm}^{-2}\text{s}^{-1}$, which seems to be a rather large value, as a Cd-ratio of more than one order of magnitude was expected instead of the observed ratio of 7.54. This would suggest that the average wavelength differs from $1.81\ \text{\AA}$. The low Cd-ratio might be attributed to the simple circular aperture of $25\ \text{mm}$ in diameter made from borated rubber, which blocks thermal neutrons except for the opening of the aperture, but allows for transmission of epithermal neutrons for a larger beam cross section of $23 \times 18\ \text{cm}^2$. Considering these $414\ \text{cm}^2$ as a source area of the epithermal neutrons and the cross section of the aperture of only $4.91\ \text{cm}^2$ as a source area for thermal neutrons would result in an additional factor of 84.3 and an effective Cd-ratio of $6.36 \cdot 10^2$. It is, therefore, most likely that the simple aperture was altering the ratio of the two neutron energy ranges of the incident neutron beam in advance for the epithermal neutrons. In order to make use of the epithermal flux available at

NECTAR it is considered to include a movable Cd-filter in the modular collimator. In combination with other filters this would result in a kind of multi filter like functionality [6].

5. Conclusions and future applications

The outcome of the measurements using a preliminary setup with an L/D ratio of 240 for thermal neutron imaging at NECTAR is very promising. The maximum spatial resolution of 88.2 μm (5.66 lp/mm) is mainly determined by the detector system at least for standard-sized samples. Larger L/D ratios provided by the modular collimator will keep the geometrical blurring comparable to the blurring caused by the scintillator, when higher spatial resolution is required at extended sample to detector distances. The integral thermal neutron flux of $7.92 \cdot 10^6 \text{ cm}^{-2} \text{ s}^{-1}$ determined by Au-foil activation is in agreement with the flux expected from the response of the employed imaging detectors. The Cd-ratio and the energy distribution at the beam port SR10 depend sensibly on the chosen aperture or collimator layout and have to be determined again for the final layout. For the employed detector configuration a rather large contamination of hot spots due to gamma rays was observed. Even with lead shielding placed around the detector gamma spots were still observed in the images. Therefore, efficient shielding is a major aspect for the design of the upgraded and the new detector system. In parallel the origin of the gamma background has to be investigated. On the one hand, there is a basic contribution of gamma radiation in the direct beam; on the other hand there are several secondary gamma radiation sources due to interactions of neutrons with structural material like the flight tube, the sample, the mirror inside the detector box, the beam stop etc. A final version of the beam collimation setup and the flight tube should minimize these contributions, e.g. by avoiding that neutrons reach the walls of the flight tube. The contribution of gamma radiation in the direct beam and the acquired radiographs has to be investigated, both for the thermal neutron beam option and the standard fission neutron beam used at NECTAR. The outcome will influence the layout of the new collimator for a combined use with thermal and fission neutrons. Future applications of the thermal beam option at NECTAR could include dual energy experiments combining thermal and fission neutrons, e.g. for hydrogen storage materials or fuel cells. A combination of these data will benefit from the even more selective contrast for hydrogen provided by fission neutrons, while thermal neutrons will serve to reach higher spatial resolution for structure materials surrounding the hydrogen containing materials. As the investigation of lithium-ion batteries often involves highly attenuating materials, there are two benefits of the thermal beam option; an increase of the average

neutron energy compared to a thermal/cold beam will result in lower activation and increased transmission signal for the investigated samples. A narrower spectral range of the neutron energy spectrum due to the missing cold spectral part will reduce beam hardening artifacts. A combination with fission neutron data promises enhanced contrast for hydrogen containing materials, e.g. the electrolyte, and thereby, enabling to follow the electrolyte distribution during battery operation. Irradiation of samples, e.g. check of radiation hardness of integrated circuits, could be carried out using both thermal and fission neutrons at a single instrument. Up to now the whole equipment for such irradiation tests has to be moved from one instrument to another one. Same is true for detector development, where the accessibility of two quite different neutron spectra may be used to evaluate detector efficiencies for various neutron energies or to simulate background effects, e.g. thermal neutron contribution to fission neutron tomography, or vice versa.

Acknowledgements

We gratefully acknowledge BMBF for funding the Thermal Neutron Beam Option at NECTAR in the frame of research project 05K16VK3.

References

- [1] M. Schulz, B. Schillinger, ANTARES: cold neutron radiography and tomography facility, *J. Large-Scale Res. Facil.* 1 (2015) A17. <https://doi.org/10.17815/jlsrf-1-42>.
- [2] T. Bücherl, S. Söllradl, NECTAR: radiography and tomography station using fission neutrons, *J. Large-Scale Res. Facil.* 1 (2015) A19. <https://doi.org/10.17815/jlsrf-1-45>.
- [3] T. Bücherl, C. Lierse von Gostomki, H. Breikreutz, M. Jungwirth, F.M. Wagner, NECTAR-A fission neutron radiography and tomography facility, *Nucl. Instrum. Methods Phys. Res. A* 651 (2011) 86–89.
- [4] E.H. Lehmann, P. Vontobel, G. Frei, G. Kuehne, A. Kaestner, How to organize a neutron imaging user lab? 13 years of experience at PSI, CH, *Nucl. Instrum. Methods Phys. Res. A* 651 (2011) 1–5.
- [5] C. Genreith, MEDAPP: fission neutron beam for science, medicine, and industry. *J. Large-Scale Res. Facil.*, 1, A18. <https://doi.org/10.17815/jlsrf-1-43>.
- [6] K. Lorenz, E. Calzada, M.J. Mühlbauer, B. Schillinger, M. Schulz, K. Zeitlhack, The new multi-filter at ANTARES: TOF measurements and first applications, in: *Proceedings of the Eighth World Conference on Neutron Radiography*, Gaithersburg, MD, USA, 2006.
- [7] M.J. Mühlbauer, E. Calzada, B. Schillinger, Development of a system for neutron radiography and tomography, *Nucl. Instrum. Methods Phys. Res. A* 542 (2005) 324–328.
- [8] M. Hoelzel, A. Senyshyn, O. Dolotko, SPODI: high resolution powder diffractometer, *J. Large-Scale Res. Facil.* 1 (2015) A5. <https://doi.org/10.17815/jlsrf-1-24>.
- [9] A. Senyshyn, M.J. Mühlbauer, O. Dolotko, M. Hofmann, T. Pirling, H. Ehrenberg, Spatially resolved in operando neutron scattering studies on Li-ion batteries, *J. Power Sources* 245 (2014) 678–683.